Chemically enhanced physical vapor deposition of tantalum nitride-based films for ultra-large-scale integrated devices

Ning Li and D. N. Ruzic[a)]
Plasma Material Interaction Group, Department of Nuclear, Plasma and Radiological Engineering, University of Illinois, Urbana, Illinois 61801

R. A. Powell
Novellus Systems, Inc., San Jose, California 95134

(Received 11 June 2004; accepted 30 August 2004; published 15 November 2004)

Physical vapor deposition (PVD) using ionized metal plasmas (ionized PVD or IPVD) is widely used to deposit conducting diffusion barriers and liners such as Ta and TaN for use in ultra-large-scale integrated (ULSI) interconnect stacks. Ionized PVD films exhibit the low resistivity, high density, and good adhesion to underlying dielectric desired for this application. On the other hand, extending PVD beyond the 45 nm technology node is problematic since IPVD may not provide sufficient step coverage to reliably coat features having high aspect ratio and sub-100 nm dimensions. Alternatively, chemical vapor deposition (CVD) and atomic layer deposition (ALD) can be used to deposit highly conformal metal films, but the electrical performance and interfacial quality may not equal that of PVD. To address future ULSI barrier/liner deposition needs, a method providing PVD-like film quality and CVD-like step coverage would be highly attractive. We have recently reported a hybrid approach to film deposition, referred to as chemically enhanced physical vapor deposition (CEPVD), in which a chemical precursor is introduced at the substrate during IPVD to provide a CVD component to the overall deposition process. The isotropic precursor flux is intended to provide film deposition on surfaces that are not impacted by the directional ions, such as the lower sidewall of a narrow via or trench. Conversely, the kinetic energy delivered to the surface by the flux of ionized metal may serve to enhance the desorption of CVD byproducts, reduce incorporation of impurities, and increase film density. In order to investigate the potential of CEPVD to deposit barrier/liner films, we have focused on the Ta-N material system since Ta/TaN is widely used as a diffusion barrier in Cu damascene processing. IPVD TaN films were deposited by reactive sputtering of a Ta target in Ar/N_2 using a planar magnetron and internal rf coils to provide a secondary ionization plasma for the sputtered neutrals. CEPVD was carried out by introducing a Ta-containing, organometallic precursor [*tert*-butylimino tris(diethylamino) tantalum] in the vicinity of the substrate surface during IPVD. Film thickness and step coverage were determined by cross-sectional scanning electron microscopy (SEM). Film composition, chemical state, and crystal structure were characterized using Auger electron spectroscopy, x-ray photoelectron spectroscopy, and x-ray diffraction, respectively. Resistivity was measured by four-point probe. Cross-sectional SEM showed improved step coverage over IPVD TaN. CEPVD film properties were highly process dependent; however, unlike IPVD TaN_x films that vary in stoichiometry but not purity, CEPVD "TaN" films contained relatively large amounts of carbon (~30%–60%) and could best be described as TaC_xN_y. Resistivity as low as ~370 $\mu\Omega$ cm was obtained for planar films of approximately 90 nm in thickness. © *2004 American Vacuum Society.*
[DOI: 10.1116/1.1808744]

I. INTRODUCTION

Copper has successfully replaced Al as a primary interconnect metal in high-speed, ultra-large-scale integrated (ULSI) circuits due to its lower electrical resistivity and higher resistance to electromigration failure. On the other hand, under the application of an electric field, Cu tends to diffuse quickly through intermetal dielectrics and can degrade their breakdown voltage. At the device level, Cu also diffuses quickly through gate oxides forming Cu-Si compounds like η''-Cu_3Si at temperature as low as 200 °C and consequently degrading device performance by forming deep level acceptors.[1,2] Therefore an effective diffusion barrier layer between the intermetal dielectric (e.g. SiO_2) and interconnect metal (Cu) is necessary. Diffusion barrier layers are usually made from metal-containing compounds or metals themselves, such as W, Ta, Ti, and nitrides of these. Ideally the layer should have continuous coverage, dense microstructure and a smooth surface morphology free of microdefects[3] in order to maintain their effectiveness with minimal occupied volume in fine features. More generally, as device features shrink down below 100 nm, there is little room for imperfection in the liner deposition. The challenge is particularly great in the case of trenches or vias with high

[a)]Electronic mail: druzic@uiuc.edu

aspect ratio (AR), for which getting satisfactory coverage of the bottom and the lower sidewall is highly demanding. Moreover, to meet the requirement of advanced dual damascene processing, the liners should also have high purity, good growth and adhesion on underlying low-dielectric-constant (low-*k*) dielectrics, etch stops, SiO_2, and Cu at deposition temperature lower than 400 °C, and compatibility with chemical mechanical planarization.

Prevalent deposition methods for barriers—including ionized physical vapor deposition (IPVD), chemical vapor deposition (CVD), and atomic layer deposition (ALD)—employ quite different growth mechanisms, sources, and process conditions, and result in distinct film properties. By utilizing the impact of energetic ion bombardment on the depositing film, IPVD can usually produce metal films with high density, smooth morphology, high purity, and low resistivity.[1,4–7] However, IPVD has difficulty in directly coating the corner and lower part of the sidewall due to the line-of-sight limit on flux into narrow trenches or vias.[3,8] In contrast, CVD and ALD offer the intrinsic capability of generating highly conformal layers even in extremely aggressive features ($AR > 10$).[9–11] However, the relatively high thermal budget of CVD and the relatively low deposition rate of ALD may limit their manufacturing application in future technology nodes. Plasma-enhanced CVD (PECVD) can be used to lower CVD deposition temperature while preserving conformal deposition, but usually results in higher impurity levels from the decomposition of the metal-containing inorganic or organic precursors (e.g., hydrocarbons, O, F, Cl). Incorporated in the layers during deposition, these impurities can degrade layer performance, resulting in higher resistivity, reduced hardness and adhesion, etc. CVD is also prone to generating particles through gas phase nucleation.

To address the limitations of conventional thin-film barrier deposition methods, we are developing an innovative technology that we have named chemically enhanced physical vapor deposition (CEPVD). This technology attempts to grow films with excellent quality as well as conformal coverage by combining the best attributes of PVD and CVD into a single hardware system and a single process step.

Extensive efforts have investigated many materials in an effort to identify an optimum barrier layer for Cu metallization, including: Cr, W,[12] MoN,[13] WN,[13] Pt, Ni, and Pd, TiN, TiW,[14] Ta,[1,4] TaN, TaSiN,[15] and TaCN.[16] Tantalum nitride has received the most attention in industrial application and research due to its high thermal stability, chemical inertness, and resistance to Cu diffusion.[1,9]

In principle, CEPVD should be capable of depositing any material that can be deposited by both CVD and PVD methods. Since tantalum nitride has been successfully deposited by PVD and CVD and proved to be an excellent candidate diffusion barrier in Cu-based ULSI metallization, we have chosen to demonstrate feasibility for the CEPVD concept using tantalum nitride as a test vehicle. We believe this work (preliminary results reported in Refs. 17–19) represents a significant effort to synergistically combine PVD and CVD technologies.

In the present work, the CEPVD experiments were implemented in an IPVD-based process chamber by attachment of a chemical precursor delivery tube. Reactive sputtering of a Ta target in an Ar/N_2 plasma supplied the physical flux component to the film. Simultaneously, an organometallic precursor vapor, *tert*-butylimino tris(diethylamino) tantalum, or TBTDET, was decomposed on the substrate surface at elevated temperature, providing the chemically produced tantalum nitride to the film. A secondary plasma is generated between the target and the substrate with an rf coil in order to ionize the sputtered metal atoms as well as promote the chemical reactions. Generally, organometallic molecules immersed in a plasma create a complex organic environment due to their complex molecular structure and the relatively loose bonds linking the respective constituent atoms: carbon, hydrogen nitrogen, metal, etc. Therefore, it was anticipated that the CEPVD films deposited in this work would contain measurable amounts of carbon and/or hydrocarbons in addition to tantalum and nitrogen. Similarly, plasma-assisted ALD "TaN" films have been reported to contain appreciable amounts of incorporated C associated with the organometallic precursor.[10,20]

The present article reports experimental properties of CEPVD TaN films and compares them with data on similar films deposited by IPVD and PECVD using the same hardware but with suitably modified configuration. For example, for CEPVD both the magnetron and the secondary rf plasma are energized, while for PECVD the magnetron is turned off. Measured film properties included thickness and step coverage by cross-sectional scanning electron microscopy (SEM), sheet resistance and resistivity by four-point probe, elemental concentration by Auger electron spectroscopy (AES), chemical bonding by x-ray photoelectron spectroscopy (XPS), and crystal structure by x-ray diffraction (XRD).

II. CEPVD THEORETICAL BACKGROUND

The CEPVD process is designed to merge CVD and PVD film deposition into a single process step, and a CEPVD chamber therefore has constituent hardware to enable both IPVD and PECVD (see Fig. 1). The physical component of the CEPVD TaN process is provided by sputtering of the Ta target by positive ions extracted from the primary plasma, followed by the conversion of a significant fraction of the sputtered Ta neutrals to Ta^+ by electron impact ionization in the secondary plasma. A planar magnetron in conjunction with an internal ICP coil generates the primary dc plasma and secondary rf plasma, respectively. A reactive Ar/N_2 plasma is used to sputter the Ta target and supplies nitrogen atoms to the wafer surface that combine with Ta adatoms to form TaN_x.

The chemical component of the CEPVD TaN process is utilized to improve step coverage and, in this case, is provided by the decomposition of TBTDET molecules in the vicinity of the sample surface. In this regard, H_2 plasmas and H_2/N_2 plasmas have been reported to be effective reducing agents for TBTDET, lowering the self-decomposition temperature of the molecule and the hydrocarbon impurity con-

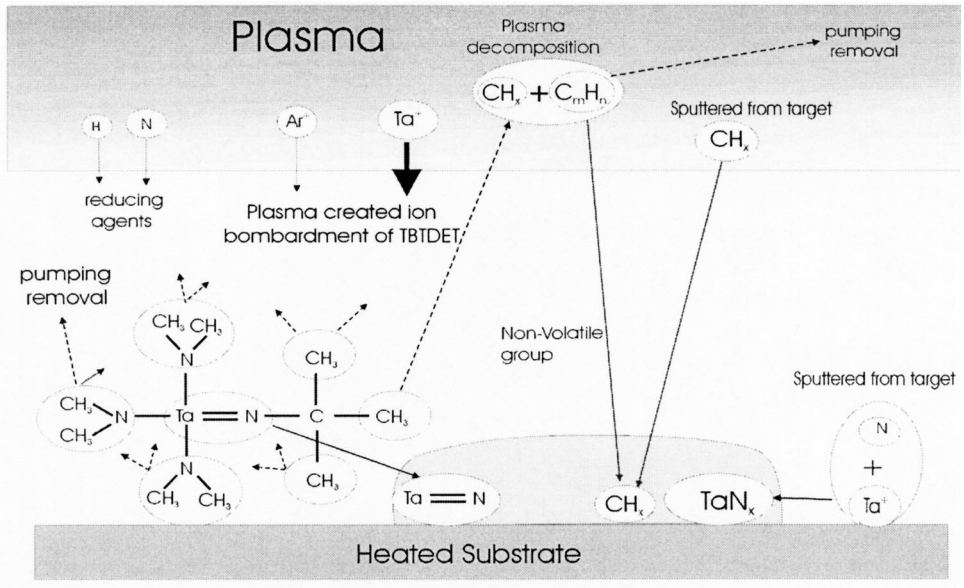

FIG. 1. Conceptual illustration of the CEPVD TaN process.

tent in the resulting TaN-based films.[10,20–23] In the present work, H_2 was introduced into the chamber during both PECVD and CEPVD to plasma-assist the decomposition of TBTDET into tantalum nitride.

The dissociation reaction of TBTDET [t-BuN $=Ta(NEt_2)_3$] results in volatilization of the organic alkyl groups and incorporation of the doubly bonded tantalum nitride moiety into the growing film (see Ref. 10). The organic products that diffuse away from the substrate surface would most likely be further decomposed in the plasma by electron impact or other collision mechanisms into smaller organic groups. Depending on their sticking coefficients, these groups could contaminate the target surface, leading to a so-called "poison mode" of operation. The poison mode is well documented in reactive sputtering of metallic targets; e.g., sputtering a Ta target in Ar/N_2 to deposit TaN. In this case, the poisoning refers to the surface nitriding of the target by N_2 from the working gas that significantly reduces the target's sputter yield and the available flux of Ta. Target poisoning in CEPVD of TaN is expected to be a much greater concern than in conventional reactive PVD because in CEPVD the target is exposed to hydrocarbon layers that are usually highly resistive and may lead to charge accumulation on the target, unstable impedance, and possible arcing. Since the steady-state hydrocarbon coverage of the Ta target is the net result of sputter etching and compound formation, the poison mode can be avoided in CEPVD by increasing the Ar sputter gas flow rate, lowering the carrier gas flow rate (i.e., reducing the flow of TBTDET), and/or reducing the diffusion of organic TBTDET breakup products to the target. In the present experiments, we have been able to adjust these conditions to maintain the target surface in the metallic mode.

A key aspect of CEPVD is the controlled, energetic ion bombardment provided by the ionized PVD component of the process. By applying a suitable negative bias to the substrate, ion energy can be adjusted from the floating potential of the substrate (~10–20 eV) to 100 eV or more. The energy provided by the incident ions is utilized to drive surface reactions and reduce the substrate temperature below that required for a purely thermal CVD process. In this sense, CEPVD is similar to ion-assisted CVD. However, in the case of CEPVD, the energetic ions include the elemental film constituents (e.g., Ta^+, N^+, and N_2^+) as opposed to being purely foreign atoms such as Ar^+ or H^+. Energetic ion bombardment during film growth can also result in preferred crystalline orientation, improved density, resistivity, and adhesion.[2,24] It should be cautioned that while ion bombardment is expected to impact film properties on the field region, upper sidewall and bottom of a high-aspect-ratio trench or via, treatment of the lower sidewall is problematic due to the highly directional nature of the ions. Experimental determination of CEPVD film properties within fine features will be needed to address this concern.

III. EXPERIMENTAL SETUP

CEPVD requires an appropriate hardware configuration providing both PVD and CVD components; however, film optimization requires that experimental parameters be chosen so that both CVD and PVD components can enhance each other. In the present work, the parameter set included dc magnetron power, secondary rf plasma power, substrate temperature, total working pressure, carrier gas and flow rate, and the relative concentration of $Ar:N_2:H_2:TBTDET$.

Experiments were carried out in a modified, commercial sputtering tool having a planar magnetron equipped with a rotating permanent magnet assembly and capable of processing 200-mm wafers (MRC Galaxy™, manufactured by Material Research Corporation, Orangeburg, NJ). A water-cooled 13.9-in.-diameter tantalum target (>99.95% purity) was used in the work reported here. Additional details of the sputtering tool are provided in Ref. 25. The process chamber was evacuated using a rotary vane roughing pump; high vacuum pumping was provided by a cryopump or turbomo-

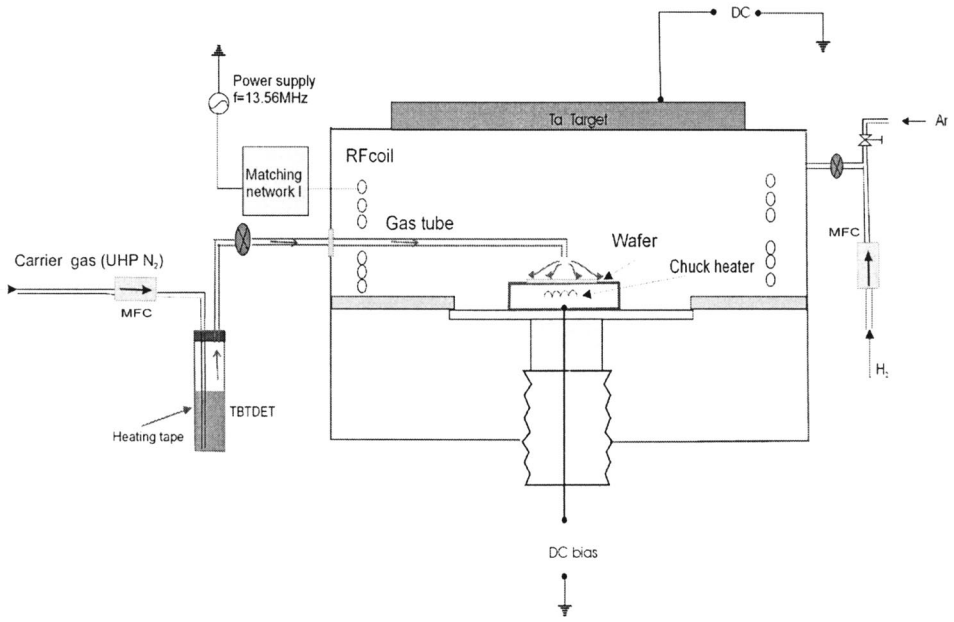

FIG. 2. Schematic diagram of the CEPVD experimental setup.

lecular pump. Base pressure was $\sim 6\times 10^{-6}$ Pa (5×10^{-8} Torr). During processing, the cryopump gate valve was closed and gas flow was maintained only by the turbopump via a throttled gate valve. Although the system is capable of coating full 200-mm wafers, substrates in the present work were typically small coupons ($\sim 3\times 3$ cm^2) cleaved from a 200 mm Si wafer with 1 μm of blanket, thermal SiO_2. Patterned coupons were also prepared to study step coverage and consisted of 1 μm thermal SiO_2 with trenches of different width and spacing etched into 1 μm of thermal SiO_2. The patterned trenches were subsequently coated with 500 Å of conformal thermal Si_3N_4 to increase their aspect ratio.

The experimental hardware was configured in such a way that IPVD, PECVD, or CEPVD could be carried out in the same process chamber by simply introducing suitable gases and powering up the appropriate plasma sources. In the IPVD experiment, Ar and N_2 were introduced into the chamber at a preset flow rate. After the pressure stabilized, magnetron power was turned on to generate the primary dc plasma. A water-cooled helical resonator coil located between the target and the substrate was driven at 13.56 MHz to generate the secondary, inductively coupled rf plasma.

The TBTDET precursor [t-BuN=Ta$(NEt_2)_3$] used in these studies was obtained from a commercial source (the Schumacher unit of Air Products and Chemicals, Carlsbad, CA) and was stored in an electropolished stainless steel bubbler wrapped by a heating tape (see Fig. 2). Ultra-high-purity N_2 was used as a push gas to deliver the TBTDET vapor from the heated bubbler. Bubbler temperature was maintained at 100 °C±5 °C for PECVD and CEPVD experiments. An ice-bath trap was connected between the turbopump and its fore line roughing pump in order to capture any unreacted TBTDET vapor. The vaporized precursor was delivered through a 1/8-in.-diameter stainless steel tube that was bent towards the wafer chuck to distribute the vapor over the sample coupon. The open end of the tube was located 0.5 cm above the chuck. In all the experiments reported here, sample coupons were placed in the same location on the wafer chuck, their center being 2 cm away from the opening of the precursor delivery tube.

The small-diameter gas delivery tube acted as a point source for the chemical component of the PECVD and CEPVD depositions. Since precursor flux decreased strongly with distance away from the tube opening, PECVD film thickness was not expected to be highly uniform over the area of the sample coupon. A similar impact of precursor delivery on the spatial uniformity of the CEPVD films was anticipated even though the large-diameter commercial magnetron source provided a uniform PVD flux over the entire 200 mm substrate holder. On the other hand, the simple delivery tube dosing scheme used here was sufficient to demonstrate proof of concept for the CEPVD process and allow comparison with IPVD and PECVD films deposited using similar hardware. Therefore, vapor delivery sources with global uniformity suitable for large-diameter wafers (e.g., extended area shower heads) were not pursued. H_2 was introduced to generate H radicals as the reducing agent for the chemical reactions. Chuck temperature was maintained at 350 °C±5 °C during the processing time for PECVD and CEPVD experiments.

The CEPVD process can be thought of as a combination of CVD and PVD, and CEPVD experiments were conducted using the same gases and plasma conditions as used for the separate IPVD and PECVD experiments. After the bubbler and wafer chuck were heated to their preset temperatures, the sputtering gas (Ar) and reducing agent (H_2) were introduced into the chamber, N_2 functioned as the carrier gas for the precursor and as a reactive gas to nitride the deposited Ta. Both primary and secondary plasmas were established prior

TABLE I. IPVD process parameters and film properties.

Experiment	Ar partial pressure (mTorr)	N_2 (sccm)	Target power (kW)	Rf power (W)	[Ta] %	[N] %	[O] %	[C] %	Thickness (nm)	Resistivity ($\mu\Omega$ cm)
IPVD	20	9	2	350	59	31	4	6	270	260

to introduction of TBTDET vapor. Chamber working pressure typically ranged from 40 to 60 mTorr and consisted of the partial pressures of Ar, N_2, H_2, TBTDET vapor, and volatile organic by-products of the deposition process. The substrate holder was electrically isolated from ground, and ion bombardment energy was varied by application of a 0–60 V negative bias voltage to the holder.

Cross-sectional SEM was used to measure film thickness and step coverage. Film resistivity was determined by the product of film thickness and sheet resistance R_s, with the latter measured by four-point probe. XRD with a copper x-ray source (Cu K_α radiation with $\lambda = 1.5405$ Å) was used to determine the crystal orientation of the deposited films. Elemental composition and chemical state were determined by AES and XPS, respectively.

IV. RESULTS

A. IPVD and PECVD planar film properties

IPVD process parameters and experimental film properties are listed in Table I. Total chamber pressure was 7 mTorr, and the substrate was at floating potential. The film contains relatively low levels of [O] and [C] impurities that we attribute to water and organic residue desorbed from the chamber walls or fixtures within the process chamber. The concentration ratio of [Ta] and [N] is 1.9, close to Ta_2N stoichiometry. While the resistivity of IPVD TaN_x films depends on both stoichiometry and thickness, the measured value of 260 $\mu\Omega$ cm is within the expected range for thick IPVD TaN_x (Ref. 26). The deposition rate was about 100 nm/min with a source-to-substrate distance of 15 cm.

PECVD films were deposited under the process conditions listed in Table II; however, in this case no dc power is applied to the magnetron. Chamber pressure was allowed to stabilize after introduction of the process gases before the secondary rf plasma was turned on. Plasma ignition occurred several seconds before the valve of the bubbler was opened to allow the chemical precursor into the chamber. Deposition rate was 50 nm/min with a total chamber pressure of 60 mTorr. The PECVD film has a carbon concentration of 54% as determined by AES. We attribute this relatively high carbon content to organic breakup products of the TBTDET molecules—both nonvolatile species and also volatile species that are not able to diffuse away from the surface boundary layer before being broken down further in the plasma under electron and ion bombardment. The XRD spectrum shows that the film (see Fig. 3) is amorphous.

B. CEPVD planar film properties

Table III lists process parameters and film properties of the CEPVD films that are identified as CEPVD (1-1), CEPVD (1-2), etc. As in the PECVD experiments, the bubbler and substrate were maintained at 100 and 350 °C, respectively, during the experiment. The magnetron was first powered up (2 kW), followed by application of rf power to the inductively coupled plasma coil and, a few seconds later, by introduction of TBTDET vapor into the process chamber. H_2 flow rate was fixed at 15 sccm, while N_2 flow rate was varied.

CEPVD (1-1) and CEPVD (1-2) were deposited with a relatively high partial pressure of sputtering gas (30 mTorr Ar) and a low carrier gas flow rate (5 sccm N_2). To avoid appreciable deposition of PVD Ta before the arrival of precursor vapor flux, target power was ramped up over a time of 1 min following precursor introduction into the chamber. The high sputtering rate of the Ta target by Ar^+ keeps the target in the metallic mode and results in a high flux of Ta and Ta^+ ions being delivered to the substrate region. Ta^+ ions are accelerated across the plasma sheath and the resulting energetic bombardment of the sample surface is expected to drive chemical reactions. Gas phase momentum transfer resulting from the same ion bombardment may also serve to inhibit the diffusion of volatile organic products away from the sample surface. On the one hand, confinement of volatile organic species near the surface would help prevent contamination of the target and the upper process chamber. On the other hand, confinement may increase the organic content in the film and may explain the high carbon concentration (61%) observed in films CEPVD (1-1) and CEPVD (1-2).

It has been reported that hydrocarbons can be converted into tantalum carbide when sufficient surface energy is

TABLE II. PECVD process parameters and film properties.

Experiment	Ar (mTorr)	H_2 (sccm)	N_2 (sccm)	Rf power (W)	[Ta] %	[N] %	[O] %	[C] %	Thickness (nm)	Resistivity ($\mu\Omega$ cm)
PECVD	20	15	10	260	22	20	4	54	190±20	32 000±3000

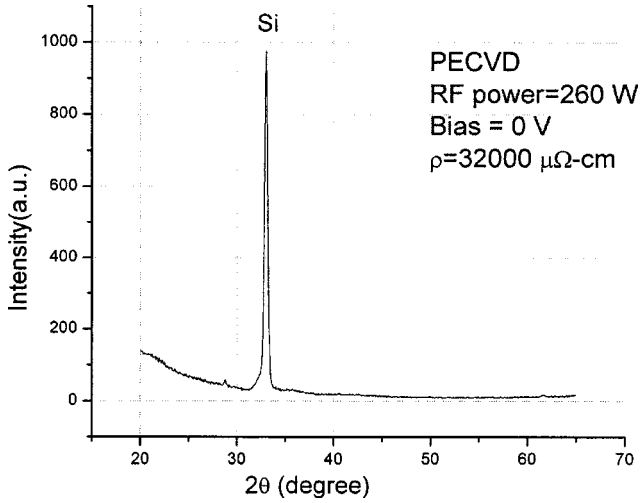

FIG. 3. XRD spectrum of PECVD film deposited under the process conditions listed in Table II.

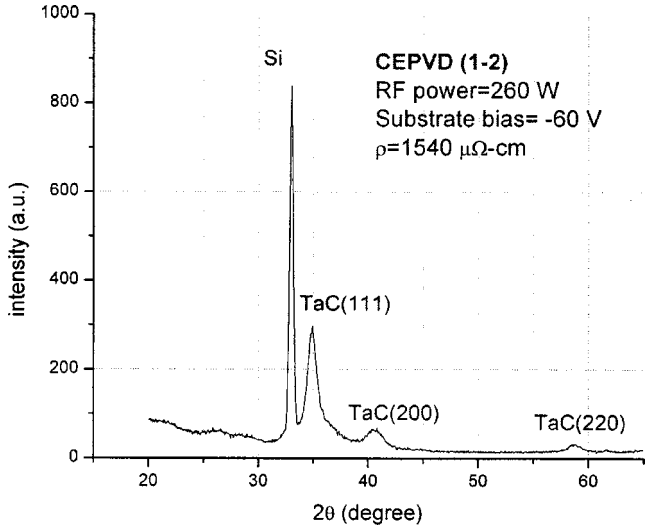

FIG. 4. XRD spectrum of experiment CEPVD (1-2) with 30 mTorr Ar and 5 mTorr N_2.

supplied.[10] This is consistent with the XRD results in Fig. 4 that show phases associated with TaC and Ta_2C. Nitrogen concentration in the film was relatively low (8%) but not unexpected given the low flow rates of N_2 and N-containing precursor used. No tantalum nitride phases were detected. The resistivity of the CEPVD film is much lower than the PECVD film but not as low as incorporated Ta_xC. Therefore, we attribute the carbon in the film to a mixture of Ta_xC and incorporated hydrocarbons.[27,28] On the other hand, the insulating hydrocarbon content of the CEPVD film may explain why its resistivity is higher than the IPVD film deposited under similar conditions.

The 60 V negative bias used for CEPVD (1-2) decreased film resistivity about 25% compared to CEPVD (1-1), but left the elemental concentration unchanged. It appears that the effect of Ta flux on the gas phase reaction and confinement has saturated despite the addition of extra kinetic energy. However, the ion bombardment is likely to encourage the formation of Ta-C bonding resulting in lower resistivity.

In contrast to the first two experiments that were done at 30 mTorr Ar partial pressure, samples CEPVD (2-1), CEPVD (2-2), and CEPVD (2-3) were deposited at a lower Ar partial pressure of 20 mTorr with 5 sccm N_2 as carrier gas, and another 5 sccm N_2 introduced directly to the chamber to provide additional reactive gas. The lower Ar pressure was expected to reduce carbon concentration in the film by increasing the diffusion length of the organic by-products and thereby more effectively removing them from the vicinity of the depositing film. Momentum transfer from the directional Ta ion flux to the wafer may also serve to confine organic by-products at the film surface, and in this regard, the lower Ta ion flux from the target at reduced Ar pressure could serve to further reduce carbon incorporation. On the other hand, since the Ar pressure directly correlates with the sputter etch rate of the target, too low an Ar pressure could lead to undesired poisoning of the Ta target by the organic by-products. With this in mind, the target power ramping time was reduced to 45 s to compensate for the weaker confinement and to keep the target from becoming contaminated. As expected, the overall carbon concentration and resistivity were reduced due to the enhancement of hydrocarbon diffusion. Nitrogen concentration in the film increased due to the additional N_2 flow rate into the process chamber. TaN phases were also detected for all three samples deposited in this group of experiments (see Fig. 5).

Rf power was increased by 50 W in CEPVD (2-2) relative to CEPVD (2-1) in order to generate a higher Ta ion flux. The film elemental concentrations were not changed, but the resistivity decreased to 370 $\mu\Omega$ cm, suggesting that tantalum

TABLE III. List of CEPVD process parameters and results. All the experiments were carried out with target power of 2 kW, H_2 flow rate of 15 sccm, and chamber pressure of approximately 40 mTorr. The baseline conditions were chosen to be those used for CEPVD (2-1).

Experiment	Ar partial pressure (mTorr)	N_2 (reactive gas) (sccm)	N_2 (carrier gas) (sccm)	Rf power (W)	Target power ramp (s)	Substrate bias (V)	[Ta] %	[N] %	[O] %	[C] %	Thickness (nm)	Resistivity ($\mu\Omega$ cm)
CEPVD (1-1)	30	0	5	260	60	0	24	8	7	61	370±20	2100±100
CEPVD (1-2)	30	0	5	260	60	−60	24	8	7	61	270±10	1500±100
CEPVD (2-1)	20	5	5	260	45	0	46	16	3	35	120±10	650±50
*CEPVD (2-2)	20	5	5	310	45	0	47	14	4	35	100±8	370±30
CEPVD (2-3)	20	5	5	310	45	−60	56	11	3	30	150±8	410±20

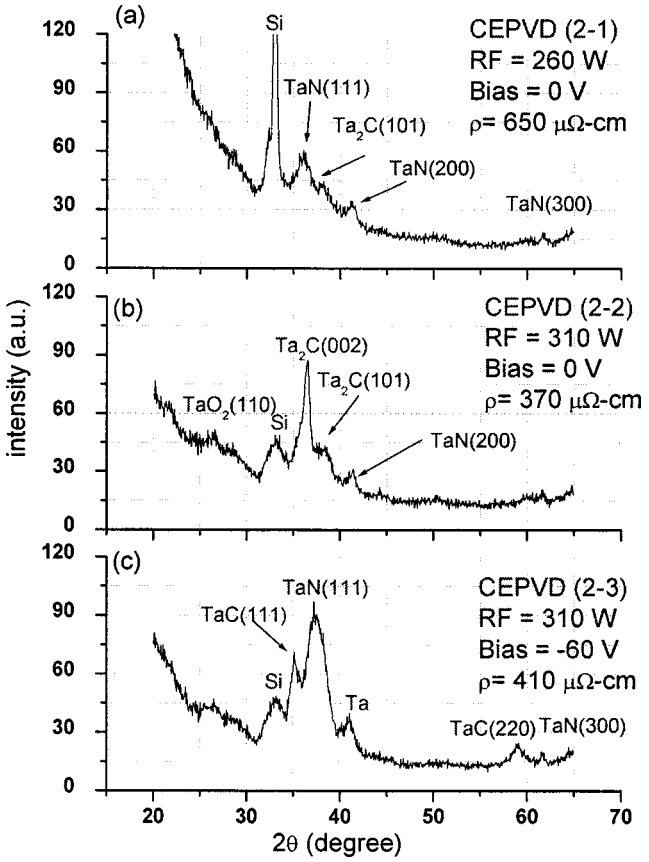

FIG. 5. XRD spectra of CEPVD experiment at 20 mTorr Ar and 10 mTorr N_2. (a) CEPVD (2-1). (b) CEPVD (2-2). (c) CEPVD (2-3).

carbide represents a larger fraction of the C concentration in the film. As shown in Figs. 5(a) and 5(b), the major XRD peak shifts from TaN (111) to $Ta_2C(002)$. In CEPVD (2-3), a negative 60 V bias was applied to the chuck to further increase the ion energy delivered to the film surface. This resulted in an XRD spectrum with TaN (111) as the dominant peak [see Fig. 5(c)] and a resistivity of 410 $\mu\Omega$ cm that was slightly higher than the 370 $\mu\Omega$ cm value for CEPVD (2-2).

Figure 6 shows high-resolution XPS spectra of sample CEPVD (2-2). The spectra confirm that Ta is bonded to nitrogen, oxygen, and carbon (peak assignments were determined using the *NIST XPS Data Base*). Figure 6(b) indicates two binding energy states for the C 1*s*; 285.13 and 282.14 eV. Although the higher energy peak is close to that of elemental carbon, we believe it unlikely that C would exist in this form considering the complexity of the chemical reactions involved. We therefore associate the higher energy peak with the presence of hydrocarbons.

C. Step coverage of trench linings

Figure 7 compares the step coverage for IPVD, PECVD, and CEPVD films deposited on trenches under similar deposition conditions (see Table IV). These experiments were designed to investigate the relative importance of the physical and chemical components of the CEPVD process.

For the IPVD experiment, process parameters were kept the same as for the CEPVD experiment (baseline case), except that the N_2 flow did not go through the TBTDET bubbler. As a result, the same amount of N_2 flowed into the chamber during both the IPVD and CEPVD experiments, but in the former case without introducing the chemical precursor. Therefore, the physical component of the CEPVD trench liner deposition was equivalent to that of the corresponding IPVD experiment. Similarly, the PECVD experiment differed from the CEPVD experiment in that the magnetron power was turned off, so that the chemical component of the two processes was equivalent.

Figure 7(a) shows that, within the resolution of the SEM image, the IPVD film had no detectable coverage on either the bottom or on the lower sidewall of an AR=7 trench (thickness on the field ~80 nm). On the other hand, the PECVD film [Fig. 7(b)] had a measurable and conformal

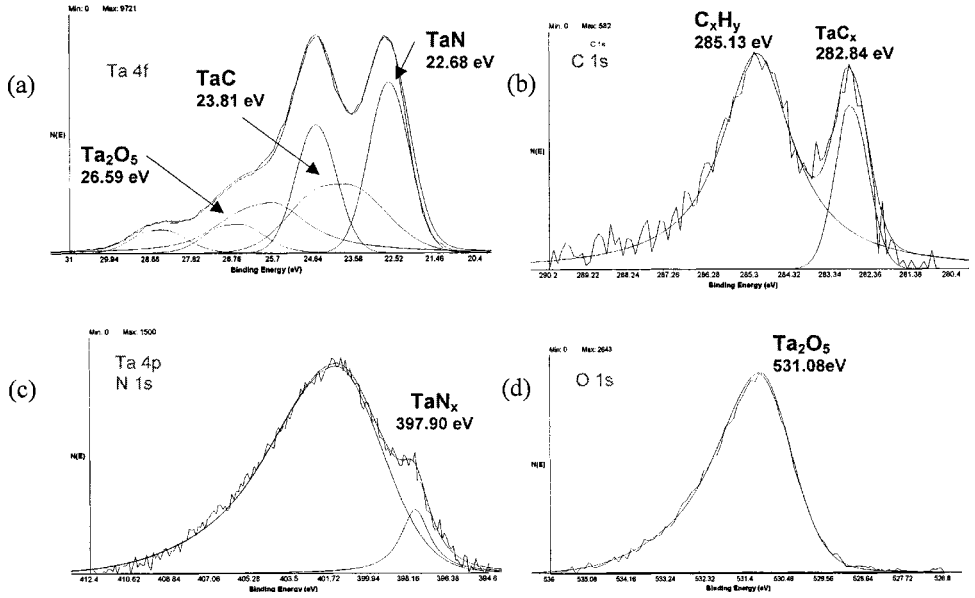

FIG. 6. High-resolution XPS spectra of CEPVD (2-2). (a) Ta 4*f*. (b) C 1*s*. (c) N 1*s*. (d) O 1*s*.

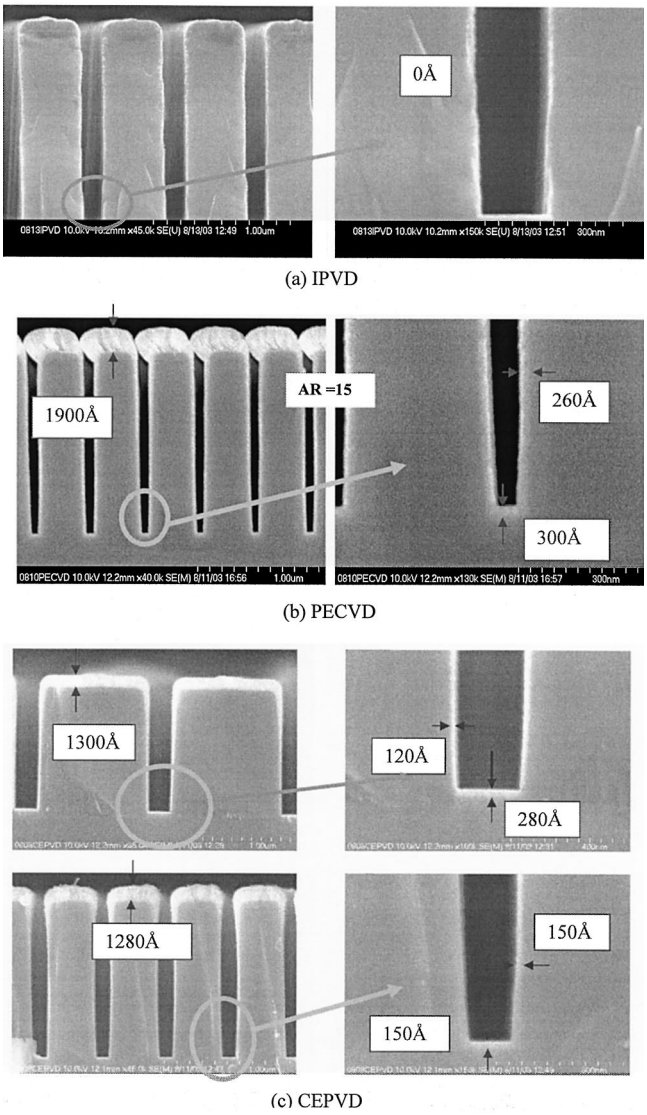

FIG. 7. Comparison of step coverage for (a) IPVD, (b) PECVD, and (c) CEPVD trench liners deposited under similar process conditions.

coverage of ~15% on the bottom and along the sidewall of a much higher aspect ratio trench (AR=15). The CEPVD film [Fig. 7(c)] had comparable coverage with the PECVD film, being about 12% for an AR=13 trench.

The submicron dimensions of the trench are too small for the plasma sheath to penetrate. As a result, ion bombardment is limited to the direction normal to the trench bottom. Resputtering of the trench bottom may have redistributed material to the lower corner sidewall; however, this would not explain the improved coverage of the CEPVD film higher up the wall. We suggest that the increased film thickness in this location resulted from thermal CVD associated with the chemical component of the CEPVD process. In effect, CVD was being used to build up material in areas that would be sparsely coated by an IPVD process alone. CEPVD film resistivity was characterized using planar films and found to be ~650 $\mu\Omega$ cm; however, this value may not be appropriate within microstructures such as a high-aspect-ratio trench or via due to the different relative contributions of the chemical and physical components of the CEPVD process.

V. CONCLUSION

In summary, experiments have been carried out in a modified, commercial PVD reactor to determine the feasibility of the CEPVD concept on TaN-based films that are of potential interest as diffusion barriers and liners. Planar CEPVD films have been obtained with resistivity as low as 370 $\mu\Omega$ cm, which is close to the resistivity of an IPVD TaN film deposited in the same chamber. Compared to IPVD films deposited on high-aspect-ratio trenches (1 μm deep, AR~13), CEPVD films exhibited improved step coverage (bottom coverage ~12%, side wall coverage ~12%), that was comparable to the coverage of PECVD films deposited in the same chamber. Adjusting process conditions so as to promote tantalum carbide formation and desorption of hydrocarbons led to decreased film resistivity. On the other hand, compared to TaN films deposited by IPVD, CEPVD "TaN" films had appreciable amounts of carbon (~30–60 at. % depending on process conditions) associated with carbide phases such as TaC and Ta_2C or with hydrocarbon incorporation. These experiments have demonstrated that the PVD and CVD components of the CEPVD process can be adjusted to produce films with lower resistivity than PECVD and higher step coverage than IPVD. Increasing the energy and flux of the incident ions to the substrate surface appears to have had two effects: (1) confinement of organic molecules at the substrate surface that served to keep the target in the metallic sputter-

TABLE IV. Process parameters for trench liners deposited by CEPVD, IPVD, and PECVD. Process conditions of the IPVD experiment were the same as for the CEPVD experiment (baseline case); however, for IPVD the N_2 flow was not introduced through the bubbler so that the same amount of N_2 could be delivered into the chamber without introducing any precursor. Experimental conditions for the PECVD experiments were the same as for CEPVD except that no dc power was applied to the PVD target.

Experiment	Ar (mTorr)	H_2 (sccm)	N_2 (sccm)	Target power (kW)	Target power ramp (sec.)	Rf power (W)	Bias voltage (V)	Chamber pressure (mTorr)
IPVD	20	15	10	2	45	260	0	40
PECVD	20	15	10	NA	45	260	0	40
CEPVD	20	15	10	2	45	260	0	40

ing mode, and (2) conversion of hydrocarbons on the substrate into tantalum carbide. The barrier performance of the CEPVD films is currently being measured and will be reported in a future communication. Characterization of film composition and resistivity within the trench also will need to be determined to fully assess the ability of CEPVD to provide robust diffusion barriers and liners.

ACKNOWLEDGMENTS

The authors would like to acknowledge the Semiconductor Research Corporation (SRC task ID. 1035.01) and Novellus Systems for providing customized SRC funding for this research. AES, XRD, XPS, and SEM were carried out in the Center for Microanalysis of Materials, University of Illinois, which is partially supported by the U.S. Department of Energy under Grant No. DEFG02-91-ER45439. We also wish to thank the undergraduate helpers, Paul Brenner, Crystal Manohar, Hussain Nomanbhai, and Ying Wu for their experimental efforts and data analysis.

[1]K. Holloway, J. Appl. Phys. **11**, 71, (1992).
[2]S. S. Wong, C. Ryu, H. Lee, and K.-W. Kwon, Mater. Res. Soc. Symp. Proc. **514**, 75 (1998).
[3]Y. Shacham-Diamond, J. Electron. Mater. **30**, 336 (2001).
[4]P. Catania, J. P. Doyle, and J. J. Cuomo, J. Vac. Sci. Technol. A **10**, 3318 (1992).
[5]L. A. Clevenger, A. Mutscheller, J. M. E. Harper, C. C. Jr., and K. Barmak, J. Appl. Phys. **72**, 4918 (1992).
[6]J. S. Reid, E. Kolawa, R. P. Ruiz, and M.-A. Nicole, Thin Solid Films **19**, 236 (1993).
[7]K.-H. Min, K.-C. Chun, and K.-B. Kim, J. Vac. Sci. Technol. B **14**, 3263 (1996).
[8]G. Herdt, A. Mcteer, and S. Meikle, *Semiconductor Fabtech*, 11th ed. (1999), Sec. 7, p. 259.
[9]X. Chen, H. L. Frisch, and A. E. Kaloyeros, J. Vac. Sci. Technol. B **17**, 182 (1999).
[10]J.-S. Park, M.-J. Lee, C.-S. Lee, and S.-W. Kang, Electrochem. Solid-State Lett. **4**, C17 (2001).
[11]E. Eisenbraun, O. v. d. Straten, Y. Zhu, K. Dovidenko, and A. Kaloyeros, in *Proceedings of the 2001 IEEE International Interconnect Technology Conference* p. 207.
[12]L. S. Hung, F. W. Saris, S. Q. Wang, and J. W. Mayer, J. Appl. Phys. **59**, 2416 (1986).
[13]S. C. Sun, Performance of MOCVD Transition Metal Nitrides as Diffusion Barriers for Cu Metallization, in *Stress Induced Phenomena in Metallization: Fourth International Workshop*, edited by H. Okabayashi and P. S. Ho (Springer, Berlin, 1998).
[14]S.-Q. Wang, S. Suthar, C. Hoeflich, and B. J. Burrow, J. Appl. Phys. **73**, 2301 (1993).
[15]E. Kolawa, J. S. Che, J. S. Reid, P. J. Pokela, and M.-A. Nicolet, J. Appl. Phys. **70**, 1369 (1991).
[16]Y. Ohshita, A. Ogura, A. Hoshino, S. Hiiro, and H. Machida, J. Cryst. Growth **220**, 604 (2000).
[17]D. N. Ruzic and N. Li, in *Proceedings of the International Conference on Metallurgical Coatings and Thin Films (ICMCTF-2003)*, San Diego, CA, 28 April–2 May 2003.
[18]N. Li and D. N. Ruzic, in Proceedings of the 50th International Symposium of the American Vacuum Society, Baltimore, MD, 2–7 Nov. 2003.
[19]N. Li and D. N. Ruzic, in *Proceedings of the 49th International Symposium of the American Vacuum Society*, Denver, CO, 3–8 Nov 2002.
[20]J.-S. Park, H.-S. Park, and S.-W. Kang, J. Electrochem. Soc. **149**, C28 (2002).
[21]H. J. Jin, M. Shiratani, T. Kawasaki, T. Fukuzawa, T. Kinoshita, Y. Watanabe, K. Kawasaki, and M. Toyofuku, J. Vac. Sci. Technol. A **17**, 726 (1999).
[22]M. Shiratani, H. J. Jin, K. Takenaka, K. Koga, T. Kinoshita, and Y. Watanabe, Sci. Technol. Adv. Mater. **2**, 505 (2001).
[23]K.-N. Cho, C.-H. Han, K.-B. Noh, J.-E. Oh, S.-H. Paek, C.-S. Park, S.-I. Lee, M. Y. Lee, and J. G. Lee, Jpn. J. Appl. Phys. **37**, 6502 (1998).
[24]H.-L. Park, K.-M. Byun, and W.-J. Lee, Jpn. J. Appl. Phys., Part 1 **41**, 6153 (2002).
[25]D. B. Hayden, D. R. Juliano, K. M. Green, D. N. Ruzic, C. A. Weiss, K. A. Ashtiani, and T. J. Licata, J. Vac. Sci. Technol. A **16**, 624 (1998).
[26]C.-S. Shin, D. Gall, P. Desjardins, A. Vailionis, H. Kim, I. Petrov, and J. E. Greene, Appl. Phys. Lett. **75**, 24 (1999).
[27]T. Laurila, K. Zeng, J. K. Kivilahti, J. Molarius, and L. Suni, J. Appl. Phys. **91**, 5391 (2002).
[28]T. Laurila, K. Zeng, J. K. Kivilahti, J. Molarius, and I. Suni, Appl. Phys. Lett. **80** 938 (2001).